DOI: https://doi.org/10.62985/j.huit_ojs.vol26.no2E.388

DETERMINATION OF OPTIMAL LOCATION AND SIZE OF ELECTRIC VEHICLE CHARGING STATIONS WITH THE INSTALLATION SPACE CONSTRAINTS

Thien Vo Minh[1], Tien Doan Thi Kieu[1], Hau Nguyen Van[1], Dieu Vo Ngoc[2*]

[1]*Can Tho University of Technology, Vietnam*

[2]*Ho Chi Minh City University of Technology, VNU-HCM, Vietnam*

[*]Email: *vndieu@hcmut.edu.vn*

Received: 23 January 2026; Revised: 3 March 2026; Accepted: 25 April 2026

ABSTRACT

This study proposed an optimizer model for determining in the optimal location and size of electric vehicle charging stations (EVCSs) in a distribution network (DN) integrated with distributed generation (DG) sources, while considering installation space constraints. The objective of the proposed model is to minimize power losses and maintain voltage stability. The Mountain Gazelle Optimizer (MGO) is applied to solve the optimization problem via two scenarios: without and with consideration in installation space constraints for three specific cases: DG-EVCS fixed, DG fixed-EVCS optimal and DG-EVCS optimal. The standard IEEE 119-bus and MATLAB R2022a software in conjunction with the MATPOWER 6.0 tool are used for simulation and results output. The obtained results are compared with those of other strong optimization algorithms to evaluate the superiority of the proposed model and the MGO algorithm. The model outcomes are proposed for planning, design, and development of EVCS infrastructure are provided in the practicality.

Keywords: EV optimal placement, MGO algorithm, distributed generation, EVCS, optimal algorithms.

1. INTRODUCTION

Carbon dioxide (CO_2) emissions from anthropogenic activities have caused significant environmental impacts, contributing to the unprecedented rate of global warming observed in recent decades [1]. Consequently, the transition toward green, clean, and renewable energy sources has become an inevitable global trend. Numerous studies have demonstrated that the exploitation and utilization of renewable energy can significantly reduce greenhouse gas emissions, thereby contributing to the development of sustainable and environmentally friendly energy systems [2]. Alongside the rapid development of renewable energy, the electrification of the transportation sector particularly the widespread adoption of electric vehicles (EVs) is widely regarded as an effective solution to reduce dependence on fossil fuels, mitigate greenhouse gas emissions, and improve overall energy efficiency [3]. However, the large scale deployment of EVs necessitates the corresponding development of charging infrastructure, in which EVCSs play a pivotal role. If EVCSs are not properly planned and operated, they may introduce adverse impacts on DNs, including voltage instability, peak load increase, harmonic distortion, and power quality degradation [4]. Therefore, it is essential to investigate and propose appropriate technical solutions to mitigate these negative effects.

In recent years, various approaches have been proposed to address the planning and operation of EVCSs. Some studies focus on EVCS location planning based on points of

interest and geographical attributes [5], while others employ machine learning techniques and graph neural networks to optimize charging station deployment in complex urban environments [6]. In addition, multi criteria decision making methods have been applied to select suitable EVCS locations in specific regions, such as the case study conducted in Cuenca, Ecuador [7]. From another perspective, the optimization of charging strategies and EV users' travel routes has been investigated to balance load demand and enhance the operational efficiency of EVCSs [8]. Beyond conventional planning methods, intelligent optimization and meta-heuristic algorithms have been widely applied to EVCS related problems. Multi objective particle swarm optimization (MPSO) has been employed to simultaneously optimize the locations and charging/discharging capacities of EVCSs in residential and commercial areas [9]. In [10], a binary random dynamic arithmetic optimization algorithm (BRDAOA) was proposed to determine optimal EVCS locations, demonstrating superior performance in reducing power losses compared to PSO, AOA, and several other meta-heuristic approaches. Furthermore, the integration of DG with EVCSs has been recognized as an effective solution to reduce power losses and improve voltage profiles, where the whale optimization algorithm (WOA) was utilized to identify the optimal placement of EVCSs and DG units [11].

The studies have been had further extended the scope of the problem by integrating EVCSs with auxiliary devices and advanced technologies. In India, the study in [12], proposed the integration of distribution static compensators (DSTATCOMs) with EVCSs to mitigate the adverse impacts of charging stations on DNs, where the optimal locations of both DSTATCOMs and EVCSs were determined using the bald eagle search algorithm (BESA). The integration of vehicle-to-grid (V2G) technology was investigated in [13], aiming to reduce active power losses, maximize economic benefits, and improve system reliability through a hybrid optimization approach combining the grey wolf optimizer (GWO) and particle swarm optimization (PSO). In [14], EVs shunt capacitor banks, and DG units were optimally placed using a combination of voltage stability indices and the marine predators algorithm, demonstrating significant improvements in power loss reduction and voltage quality enhancement. The integration of renewable energy sources with EVCSs has also attracted considerable attention. An improved Harris hawks optimization algorithm was proposed in [15], to optimally coordinate hybrid renewable energy sources, such as photovoltaic (PV) and wind systems, for EVCS applications, thereby enhancing energy management efficiency and reducing operational costs. In addition, a PV system combined with battery energy storage was proposed in Brazil to mitigate the long term impacts of EV penetration on DNs [16]. Moreover, several studies have focused on multi-objective optimization problems related to EVCSs, notably employing NSGA-II and MOEA/D to optimize the capacities of EVCS systems integrated with solar energy, hydrogen, and battery storage technologies. Notably, the work in [17] adopted a comprehensive approach to PV integrated EVCS systems, including optimal system design, energy yield assessment, technical performance evaluation, and economic analysis. However, this study primarily focused on the charging station level, while the impacts on DN operation, power losses, and technical performance indices were not thoroughly investigated.

The critical review of the aforementioned studies indicates that numerous effective solutions have been proposed to mitigate the negative impacts of EVCSs on DNs, including optimal placement and sizing of EVCSs, integration of distributed generation and energy storage systems, and the application of intelligent optimization techniques. Nevertheless, most existing studies address isolated objectives, such as minimizing power losses or improving voltage profiles, whereas the simultaneous optimization of EVCS locations and capacities in conjunction with distributed generation in large scale DNs remains insufficiently explored. Furthermore, many meta-heuristic algorithms reported in the literature involve complex structures, require extensive parameter tuning, and are prone to premature convergence to local

optima, which limits their practical applicability in real world power system planning and operation. Therefore, there is a pressing need for an optimization approach with a simple structure, strong global search capability, and robust convergence performance suitable for complex distribution systems.

These challenges created motivation for proposing in the MGO application to solve the problem of optimal placement and sizing of EVCSs based on the objective of minimizing active power losses. The primary goal of the proposed approach is to reduce power losses, mitigate voltage drops, and alleviate network congestion, thereby enhancing the operational stability of the distribution system. To further improve the effectiveness of the proposed solution, distributed generation units are simultaneously integrated with EVCSs to support local loads and improve voltage quality. The proposed methodology is validated on the standard IEEE 119-bus. All simulations are conducted using MATLAB R2022a in conjunction with the MATPOWER 6.0 toolbox. To comprehensively evaluate the performance of the proposed approach, two main operational scenarios are considered. The first scenario investigates the case without charging station zoning, while the second scenario incorporates charging station zoning constraints. Within each scenario, three cases are analyzed: (i) fixed DG and EVCS capacities, (ii) fixed DG capacity with optimized EVCS capacity, and (iii) simultaneous optimization of both DG and EVCS capacities. This structured evaluation framework enables a detailed assessment of the effectiveness and robustness of the MGO algorithm under various planning and operational conditions.

The main contributions of the study can be summarized such as:

- The model of optimal location and size of EVCS with installation space constraints.
- The method of applying MGO to implement the EVCS problems.
- The simulation techniques and result retrieval used MATLAB R2022a software.
- The computational tools proposed for application in developing EVCS in practice.

2. PROBLEM FORMULATION

2.1. Minimization of active power loss

The objective function of the optimization problem is defined as the minimization of the total active power loss in the distribution system, which can be expressed as:

$$F = \min(P_{Loss}) \tag{1}$$

Where P_{Loss} denotes the total active power loss of the system and is calculated as follows:

$$P_{Loss} = \sum_{k=1}^{N_r} R_k I_k^2 \tag{2}$$

Where, k is the index of the distribution line; R_k represents the resistance of line k^{th}; I_k is the current flowing through line k^{th}, N_r denotes the total number of lines in the DN.

2.2. Constraints

Voltage limits:

The permissible voltage magnitude at each bus is constrained by:

$$V_i^{\min} \le V_i \le V_i^{\max} \qquad i = 1,2,3...,N_b \tag{3}$$

Where, $V_i^{\min}$, $V_i^{\max}$ represent the minimum and maximum allowable voltage limits, respectively, N_b denotes the total number of buses in the DN.

Power balance:

$$P_{SUB} + \sum_{j=1}^{N_{DG}} P_{DG} = \sum_{j=1}^{N_b} P_L + \sum_{j=1}^{N_{EVCS}} P_{EVCS} + \sum_{j=1}^{N_b} P_{Loss} \qquad j = 1,2,...,N_b; \tag{4}$$

$$Q_{SUB} + \sum_{j=1}^{N_{DG}} Q_{DG} = \sum_{j=1}^{N_b} Q_L + \sum_{j=1}^{N_{EVCS}} Q_{EVCS} + \sum_{j=1}^{N_b} Q_{Loss} \qquad j = 1,2,...,N_b; \tag{5}$$

Where, P_{SUB}, Q_{SUB} denote the active and reactive power supplied by the utility grid; P_{DG}, Q_{DG} represent the active and reactive power generated by DG units; P_L, Q_L denote the total active and reactive load demands of the system; P_{EVCS}, Q_{EVCS} represent the total active and reactive power demand of EVCSs; P_{Loss},, Q_{Loss} are the total active and reactive power losses of the DN.

Power capacity constraints:

$$P_{EVCS,i}^{\min} \le P_{EVCS,i} \le P_{EVCS,i}^{\max} \qquad i = 1,2,3...,n \tag{6}$$

$$P_{DG,i}^{\min} \le P_{DG,i} \le P_{DG,i}^{\max} \qquad i = 1,2,3...,n \tag{7}$$

Where, $P_{EVCS,i}^{\min}$, $P_{EVCS,i}^{\max}$ the minimum and maximum operating power of the i^{th} EVCS; $P_{DG,i}^{\min}$, $P_{DG,i}^{\max}$ denote the minimum and maximum operating power of the i^{th} DG unit; n represent the total numbers of EVCSs and DG units in the DN, respectively.

2.3. Objective Function

$$FT = F + k_1 \sum_{i=1}^{N_b} (V_i - V_i^{\lim})^2 + k_2 \sum_{i=1}^{N_b} (S_L - S_L^{\lim})^2 \tag{8}$$

Where, k_1, k_2 are penalty coefficients.

3. MOUNTAIN GAZELLE OPTIMIZER (MGO)

The MGO is a recently proposed powerful optimization algorithm introduced in 2022 by Abdollahzadeh et al. The algorithm is inspired by the social behavior and survival strategies of mountain gazelles observed in nature. MGO models four principal behavioral characteristics of mountain gazelles and translates them into mathematical operators to guide the search process toward optimal solutions.

3.1. Solitary territorial males

Upon reaching maturity, male mountain gazelles establish individual territories and remain spatially separated from other members of the herd. During this stage, younger males compete to acquire territories or mating opportunities, whereas mature males focus on defending their established territories. This behavioral pattern is mathematically modeled by Eqs (9) - (13).

$$TSM = male_{gazelle} - \left| \left(ri_1 \times BH - ri_2 \times X(t) \right) \times F \right| \times Cof_r \tag{9}$$

Where, $male_{gazelle}$ represents the global best male individual, ri_1 and ri_2 are random values uniformly distributed in the interval [0;1], *BH* denotes the coefficient vector associated with the herd of young male gazelles, which is defined by Eq. (10), the value of *F* is determined according to Eq. (11), Cof_r is a random coefficient vector that is updated at each iteration based on Eq. (12).

$$BH = X_{ra} \times \lfloor r_1 \rfloor + M_{pr} \times \lceil r_2 \rceil,\ ra = \left\{ \left\lceil \frac{N}{3} \right\rceil ...N \right\} \tag{10}$$

Where, X_{ra} is a randomly selected individual from the population, M_{pr} represents the mean position of randomly selected individuals in $\left\lceil \frac{N}{3} \right\rceil$, and *N* denotes the population size.

$$F = N_1(D) \times \exp\left(2 - Iter \times \left(\frac{2}{MaxIter}\right)\right) \tag{11}$$

Where, $N_1(D)$ denotes a random value drawn from a standard normal distribution, *Iter* represents the current iteration and *MaxIter* denotes the maximum number of iterations.

$$Cof_i = \begin{cases} (a+1) + r_3, \\ a \times N_2(D), \\ r_4(D), \\ N_3(D) \times N_4(D)^2 \times \cos\left((r_4 \times 2) \times N_3(D)\right), \end{cases} \tag{12}$$

Where r_3 and r_4 are random variables uniformly distributed in [0;1], $N_2(D)$, $N_3(D)$ and $N_4(D)$ are random parameters generated within the search space. These parameters are calculated as follows:

$$a = -1 + Iter \times \left(\frac{-1}{MaxIter}\right) \tag{13}$$

3.2. Breeding herd

The mountain gazelle population is sustained through a distinctive breeding mechanism. Female gazelles play a crucial role in nurturing and protecting the offspring, while mature male gazelles not only participate in the reproduction process but also assist younger males in competing for mating opportunities.

$$MH = \left(BH + Cof_{1,r}\right) + \left(ri_3 \times male_{gazelle} - ri_4 \times X_{rand}\right) \times Cof_{1,r} \tag{14}$$

Where, X_{rand} represents the position of a randomly selected individual within the search space.

3.3. Mature gazelle herd

Mature male gazelles are driven to establish and defend territories as well as compete for mating opportunities, while simultaneously facing challenges from emerging younger males and rival mature males. This phase is mathematically represented by Eqs. (15) and (16).

$$BMH = \left(X(t) - D\right) + \left(ri_5 \times male_{gazelee} - ri_6 \times BH\right) \times Cof_r \quad (15)$$

$$D = \left(\left|X(t)\right| + \left|male_{gazelle}\right|\right) \times \left(2 \times r_6 - 1\right) \quad (16)$$

Where ri_5 and ri_6 are random integers 1 or 2, r_6 is a random value, $X(t)$ is the current position of the vectors.

3.4. Migration for foraging

Mountain gazelles are characterized by their high running speed and exceptional jumping ability, enabling them to migrate over long distances in search of food resources. This exploratory behavior is mathematically modeled by the following equation:

$$MSF = \left(ub - lb\right) \times r_7 + lb \quad (17)$$

Where, ub and lb represent the upper and lower bounds of the decision variables, respectively.

3.5. Application of MGO for EVCS model

Steps for Applying the MGO Algorithm to Solve the EVCS Optimization Problem:

Step 1: Initialize the population parameters, including the population size $nP = 100$, the maximum number of iterations $Iter = 500$, and randomly generate the initial population.

Step 2: Check the iteration counter. If the current iteration is less than the maximum number of iterations, proceed to Step 3. Otherwise, go to Step 5.

Step 3: Check the individuals within the population. If unprocessed individuals remain, evaluate their fitness values by computing *TSM, MH, BMH, MSF* then add them to the habitat and return to Step 3. If all individuals have been evaluated, update the population as described in Step 4.

Step 4: Sort the population in ascending order of fitness according to (8), update the current best solution, store the top N best individuals in the population, and return to Step 2.

Step 5: Terminate the algorithm and extract the optimal results.

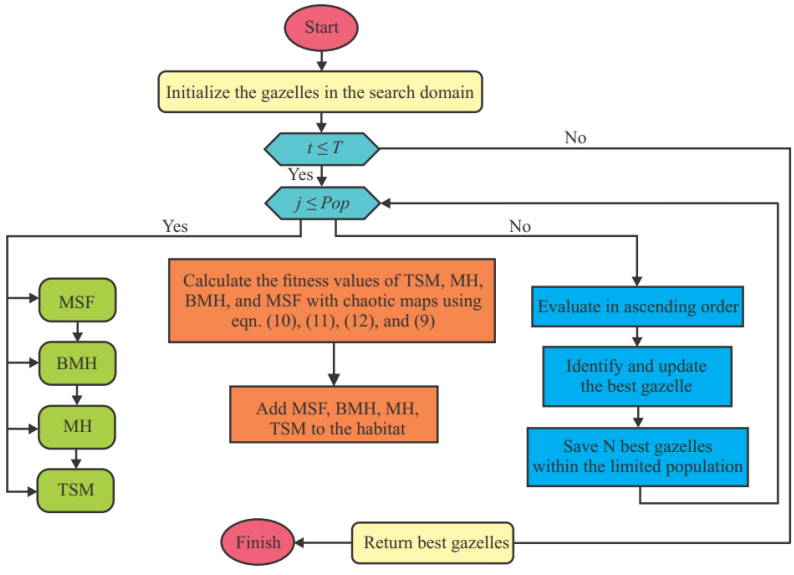

Fig. 1. Flowchart MGO algorithm

4. SIMULATION RESULTS

4.1. Input parameters

To evaluate the search capability of the proposed MGO algorithm for the EVCS location determination problem, several well established metaheuristic optimization algorithms, including NRBO, AGWOCS, GOA, GWO, CHIO, and MSA, are employed for comparison under the same problem formulation. The EVCS capacities and simulation results are presented in Table 1. The standard IEEE 119-bus DN is adopted as the test system, with the main substation located at bus 1 and a nominal voltage level of 11 kV. The total system load is 22.7 MW and 17.0 MVAr, power loss 820.8046 (kW), and the bus voltage limits are maintained within the range of 0.95 - 1.05 p.u. During the simulation process, the control parameters of all comparison algorithms are configured to ensure a fair and unbiased evaluation.

Specifically, for the CHIO algorithm [18], the population size is set to 100, the maximum age is 50, the initial coefficient $C0 = 1$, and the birth rate $BRr = 0,5$; the maximum number of iterations is set to 500. For the AGWOCS [19], NRBO, MGO [20], GOA [21], GBO [22], GWO [23], MSA [24], algorithms, the population size is also fixed at 100, and the maximum number of iterations is uniformly set to 500. The objective of the optimization problem is to minimize active power losses and bus voltage deviations through the optimal allocation of both the locations and capacities of EVCSs, while simultaneously coordinating distributed generation resources. This optimization is carried out subject to system voltage and power constraints to ensure secure and stable operation of the DN.

Table 1. Testing simulation results

Parameter	Power (MW)	NRBO (MW/bus)	AGWOCS (MW/bus)	GOA (MW/bus)	GWO (MW/bus)	CHIO (MW/bus)	MGO (MW/bus)	MSA (MW/bus)
EVCS01	1,5 ÷ 2,0	1.861 (6)	1.753 (58)	1.805 (2)	1.760 (34)	1.680 (84)	2.000 (28)	1.789 (40)
EVCS02	1,5 ÷ 2,0	1.513 (63)	1.538 (18)	1.927 (15)	1.824 (35)	1.866 (63)	1.626 (18)	1.500 (84)
EVCS03	1,5 ÷ 2,0	1.538 (64)	1.812 (5)	1.975 (4)	1.819 (5)	1.824 (38)	2.000 (3)	1.879 (3)
EVCS04	1,5 ÷ 2,0	1.877 (3)	1.500 (84)	1.668 (12)	1.989 (8)	1.907 (39)	1.558 (11)	1.683 (100)
EVCS05	1,5 ÷ 2,0	1.515 (34)	1.966 (7)	1.853 (14)	1.988 (10)	1.907 (2)	2.000 (2)	1.802 (14)
EVCS06	1,5 ÷ 2,0	1.867 (5)	1.750 (4)	2.000 (39)	1.981 (40)	1.882 (19)	1.701 (61)	1.616 (63)
EVCS07	1,5 ÷ 2,0	1.523 (16)	1.750 (9)	1.826 (7)	1.500 (15)	1.912 (34)	1.503 (56)	1.500 (2)
EVCS08	1,5 ÷ 2,0	1.885 (2)	1.750 (6)	1.500 (17)	1.530 (84)	1.878 (12)	1.897 (69)	1.500 (34)
EVCS09	1,5 ÷ 2,0	1.515 (12)	1.851 (63)	1.541 (10)	1.500 (28)	1.546 (14)	1.863 (13)	1.563 (11)
EVCS10	1,5 ÷ 2,0	1.610 (25)	1.750 (17)	1.781 (63)	1.802 (2)	1.738 (28)	2.000 (40)	2.000 (28)
EVCS11	1,5 ÷ 2,0	1.508 (56)	2.000 (12)	1.549 (6)	1.723 (56)	2.000 (6)	1.732 (4)	1.578 (65)
EVCS12	1,5 ÷ 2,0	1.816 (18)	1.750 (2)	2.000 (56)	1.999 (14)	1.979 (78)	2.000 (14)	1.704 (7)
EVCS13	1,5 ÷ 2,0	1.871 (4)	1.651 (29)	1.501 (33)	1.760 (3)	1.859 (56)	1.926 (5)	1.501 (4)
EVCS14	1,5 ÷ 2,0	1.861 (19)	1.948 (53)	1.880 (18)	2.000 (11)	1.962 (16)	2.000 (84)	1.892 (61)
Objective Function		190.1624	190.6061	185.0576	182.003	187.1574	178.6714	185.6489
CPU Time (s)		111.5762	110.9023	220.3824	110.5618	111.0686	461.1576	110.4011
Ploss (kW)		1028.6	1115.6	1018.3	1063.3	1162.3	1075.8	1026.9
Vmin (pu)		0.9433	0.9400	0.9435	0.9413	0.9377	0.9404	0.9408
VD		0.1740	0.1899	0.1722	0.1809	0.1972	0.1860	0.1779

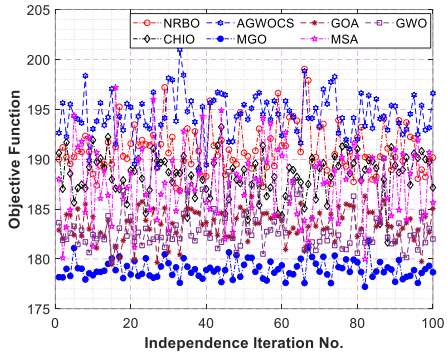

Fig. 2. Comparison based on independent runs

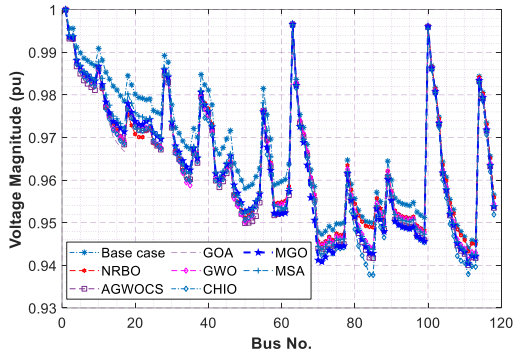

Fig. 3. Comparison of bus voltage magnitude

The simulation results presented in Table 1 and Fig. 2 indicate that the proposed MGO exhibits superior search capability compared with the other metaheuristic algorithms. Specifically, MGO achieves the lowest objective function value of 178.6714, outperforming the two closest competitors, GWO and MSA, which obtain objective values of 182.003 and 185.6489, respectively. The results obtained from 100 independent runs demonstrate that MGO not only provides high quality solutions but also exhibits strong stability and consistency, maintaining high accuracy compared to the remaining algorithms, as illustrated by the dark blue curve in Fig. 2. In addition, the minimum bus voltage reaches 0.9404 p.u, satisfying the imposed voltage constraints. The voltage profiles of all buses remain within acceptable limits throughout the entire evaluation period, as shown in Fig. 3. Although the computational time of MGO (461.1576) is slightly higher than that of some other algorithms, this drawback has a negligible impact when considering the significant improvement in solution quality. These results confirm that the proposed application of MGO to the formulated optimization model is both effective and appropriate.

4.2. Optimal location without installation space constraints

In this scenario, the optimization model for determining the optimal locations of EVCSs aims to minimize active power losses while satisfying bus voltage limits and power balance constraints. The problem is investigated through three different cases:

- Case 1: Optimal siting of EVCSs with fixed EVCS and DG capacities.
- Case 2: Optimal siting and sizing of EVCSs with fixed DG capacity.
- Case 3: Simultaneous optimal siting and sizing of both EVCSs and DGs.

In all three cases, the locations of DGs are fixed at 4, 14, 18, 34, 40, 49, 56, 61, 69, 78, 84, 91, 102 and 109. The fixed EVCS capacity is set to a nominal value of 2.0 (MW), while its optimized capacity is allowed to vary within the range of 1.0 - 2.0 (MW). Similarly, the DG capacity is fixed at 0.8 (MW) and optimized within the range of 0.1 - 0.8 (MW). The IEEE 119-bus DN is employed to perform the simulations, solution search, and result extraction using the proposed MGO algorithm, with an initial population size of $N = 100$, a maximum number of iterations $Iter_{max} = 500$, and 20 independent runs to ensure solution robustness.

Table 2. The simulation results in the optimal location without spatial constraints

Parameter	Case 01 (MW/Bus)	Case 02 (MW/Bus)	Case 03 (MW/Bus)
EVCS01	2.0 (2)	1.0 (63)	1.0 (3)
EVCS02	2.0 (56)	1.0 (5)	1.0 (4)
EVCS03	2.0 (4)	1.0 (10)	1.0 (30)
EVCS04	2.0 (28)	1.0 (6)	1.0 (14)
EVCS05	2.0 (64)	1.0 (64)	1.0 (29)
EVCS06	2.0 (63)	1.0 (28)	1.0 (5)
EVCS07	2.0 (14)	1.0 (11)	1.0 (10)
EVCS08	2.0 (3)	1.0 (47)	1.0 (28)
EVCS09	2.0 (29)	1.0 (100)	1.0 (11)
EVCS10	2.0 (10)	1.0 (4)	1.0 (2)
EVCS11	2.0 (78)	1.0 (14)	1.0 (30)
EVCS12	2.0 (65)	1.0 (56)	1.0 (40)
EVCS13	2.0 (100)	1.0 (3)	1.0 (56)
EVCS14	2.0 (40)	1.0 (2)	1.0 (6)
DG01	0.8	0.8	0.8
DG02	0.8	0.8	0.8
DG03	0.8	0.8	0.8
DG04	0.8	0.8	0.8
DG05	0.8	0.8	0.8
DG06	0.8	0.8	0.8
DG07	0.8	0.8	0.8
DG08	0.8	0.8	0.8
DG09	0.8	0.8	0.8
DG10	0.8	0.8	0.8
DG11	0.8	0.8	0.7912
DG12	0.8	0.8	0.8
DG13	0.8	0.8	0.8
DG14	0.8	0.8	0.8
Objective Function	574.9584	417.1883	420.6516
CPU Time (s)	607.8711	582.9035	586.8148
Ploss (kW)	469.0571	469.0571	469.3450
Vmin (pu)	0.9574	0.9574	0.9574
VD	0.0710	0.0710	0.0711

Based on the three simulation cases, the results presented in Table 2 indicate that the proposed MGO algorithm effectively satisfies all the imposed constraints of the optimization problem. In Cases 2 and 3, where the capacities of EVCSs and DGs are optimized, the objective function value is significantly reduced to 417.1883 and 420.6516, respectively, as

reflected by the convergence characteristics shown in Fig. 4. In contrast, Case 1, in which both EVCS and DG capacities are fixed, yields a considerably higher objective value of 574.9584. The corresponding active power losses also vary according to the power flow balance in each case, reaching 469.0571 (kW), 469.0571 (kW), and 469.3450 (kW), respectively. Meanwhile, the differences in CPU computation time among the three cases are negligible. Notably, only Cases 2 and 3 satisfy the voltage constraints effectively, with minimum voltage magnitudes of 0.9574 p.u respectively, and the lowest voltage deviations, as indicated by the red curve in Fig. 5. The voltage magnitude profile exhibits a decreasing trend toward buses located farther from the power source. Regarding EVCS siting, all three cases comply well with the problem constraints. However, the optimal EVCS locations are predominantly concentrated near the power source at 3, 4, 30 14, 29, 5, 10, 28, 11, 2, 30, 40, 56 and 6 with case 03. Although this placement strategy contributes to reducing power losses and improving voltage stability, it may introduce practical limitations in real DNs, where geographical layouts require a more spatially distributed deployment of EVCSs to ensure adequate charging service coverage.

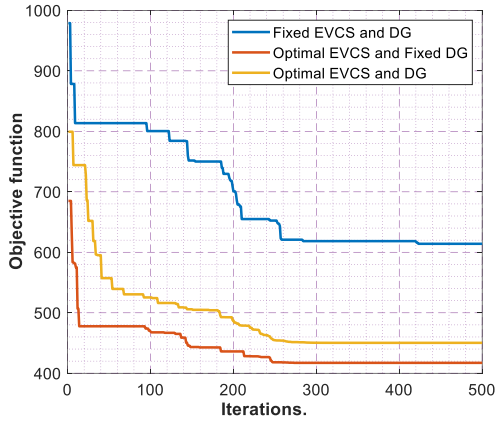

Fig. 4. Convergence characteristics

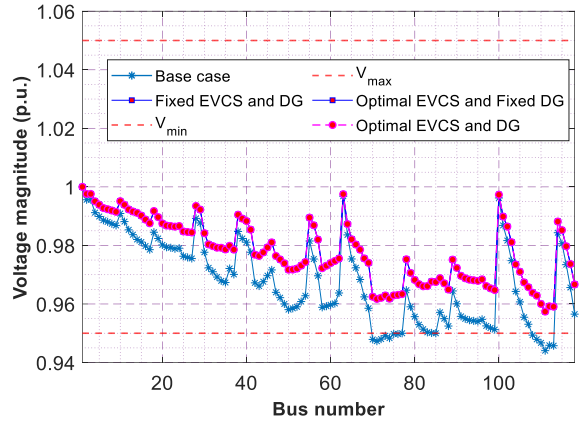

Fig. 5. Node voltage amplitude in the cases investigated

4.3. Optimal location with installation space constraints

The voltage improvement and ensure a stable distribution of EVCS power across the system, a solution considering spatial installation constraints are proposed in this scenario. The IEEE 119-bus DN is divided into three zones for EVCS deployment, with EVCS capacities allocated in a decreasing manner as the distance from the power source increases, as summarized in Table 3. The capacity of DGs is constrained within the range of 0.1 – 0.8 (MW).

Table 3. Logical zoning of the IEEE 119-bus network

Zone	Bus indices	Power limit (MW)	Electrical characteristics	Role in optimization
Zone 1	2 ÷ 55	1.5 ÷ 2.0	Close to slack bus, strong voltage profile, low power loss	Suitable for small to medium EVCS
Zone 2	56 ÷ 86	1.0 ÷ 1.5	Intermediate feeders, balanced load distribution	Candidate region for optimal EVCS placement
Zone 3	87 ÷ 119	0.5 ÷ 1.0	Electrically remote, weak voltage, high loss sensitivity	Priority area for large EVCS with DG/BESS support

Although the IEEE 119-bus system consists of 119 buses, only buses 2 to 119 are considered in the optimization space for EVCS siting in this study. This restriction is motivated

by the fact that buses with indices greater than 87 are located at the tail end of the network, where voltage levels are relatively weak, load demand is low, and voltage sensitivity is high, Therefore, the proposed EVCS capacity is also reduced to ensure the voltage remains stable at a high level (0.5 ÷ 1.0 (MW)). Installing high capacity EVCSs at these locations is likely to cause voltage constraint violations, increased power losses, and a higher risk of branch overloading.

The results presented in Table 4 and Fig. 6 further confirm the strong performance of the proposed MGO algorithm, as all three cases demonstrate good adaptability and effective satisfaction of the power balance constraints. In Cases 1 and 2, where the DG capacities are kept fixed, a reduction in EVCS capacity leads to a significant decrease in the objective function value, from 518.9050 to 434.1986, respectively. The optimized EVCS capacities tend toward their minimum limits, while the DGs are dispatched toward their maximum capacities, clearly indicating that the power balance constraints are effectively enforced to achieve objective minimization. This behavior is particularly evident in Case 3, where the EVCS capacities in all three zones reach their minimum values and the DG capacities attain the maximum limit of 0.8 (MW). As a result, the objective function value is reduced to 429.7326, with total power losses of 376.4726 (kW) and the highest minimum voltage magnitude of 0.9703 p.u. among the three investigated cases, as illustrated by the red curve in Fig. 7. The optimal EVCS locations are identified at buses 14, 2, 28, 6, 3, 41, 36, 44, 58, 43, 94, 82, and 81. These results demonstrate that spatially distributed EVCS power allocation across different zones enables improved power balance, more effective DG utilization, and most importantly, enhanced and sustained bus voltage profiles throughout the entire DN.

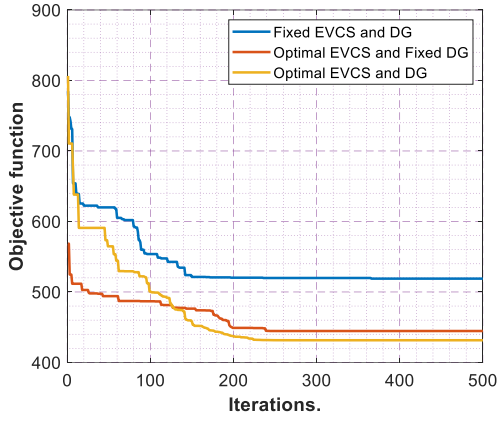

Fig. 6. Convergence characteristic of three cases

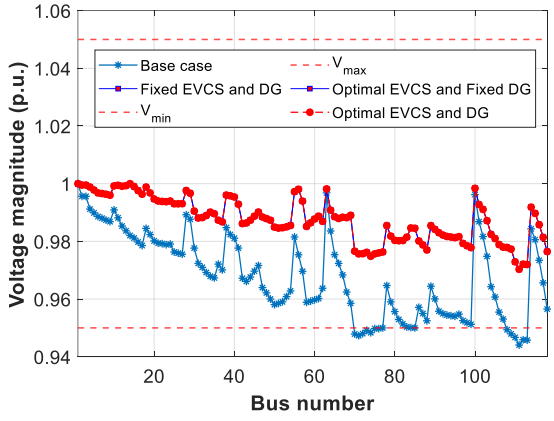

Fig. 7. Voltage magnitude via three constrained cases

Table 4. Simulation results for the three cases with spatial installation constraints

Parameter	Case 01(MW/Bus)	Case 02 (MW/Bus)	Case 03 (MW/Bus)
EVCS01	2.0 (2)	1.5 (14)	1.5 (14)
EVCS02	2.0 (14)	1.5 (35)	1.5 (2)
EVCS03	2.0 (28)	1.5 (18)	1.5 (28)
EVCS04	2.0 (3)	1.5 (2)	1.5 (6)
EVCS05	2.0 (10)	1.5 (3)	1.5 (3)
EVCS06	1.5 (36)	1.0 (43)	1.0 (41)
EVCS07	1.5 (41)	1.0 (64)	1.0 (36)
EVCS08	1.5 (44)	1.0 (41)	1.0 (44)
EVCS09	1.5 (43)	1.0 (36)	1.0 (58)
EVCS10	1.5 (58)	1.0 (44)	1.0 (43)
EVCS11	1.0 (83)	0.5 (80)	0.5 (94)
EVCS12	1.0 (81)	0.5 (82)	0.5 (82)
EVCS13	1.0 (82)	0.5 (81)	0.5 (81)
EVCS14	1.0 (80)	0.5 (83)	0.5 (80)
DG01	0.8	0.8	0.8
DG02	0.8	0.8	0.8
DG03	0.8	0.8	0.8
DG04	0.8	0.8	0.8
DG05	0.8	0.8	0.8
DG06	0.8	0.8	0.8
DG07	0.8	0.8	0.8
DG08	0.8	0.8	0.8
DG09	0.8	0.8	0.8
DG10	0.8	0.8	0.8
DG11	0.8	0.8	0.8
DG12	0.8	0.8	0.8
DG13	0.8	0.8	0.8
DG14	0.8	0.8	0.8
Objective Function	518.9050	434.1986	429.7326
CPU Time (s)	209.3904	246.1155	224.6313
Ploss (kW)	376.4726	376.4726	376.4726
Vmin (pu)	0.9703	0.9703	0.9703
VD	0.02528	0.02528	0.02528

4.4. The discussion problems of EVCS models

Based on the simulation scenarios are demonstrated the MGO algorithm effectively satisfies the requirements of the proposed optimization problem. The results obtained from the investigated cases demonstrate strong adaptability to variations in power flow conditions and problem constraints, with MGO consistently providing accurate and reliable solutions across all scenarios. The identification of optimal EVCS locations is significantly improved when spatial installation constraints are introduced into the system. This outcome confirms the suitability of the proposed approach for real world DNs, where EVCS deployment must comply with specific geographical and zoning requirements. Furthermore, the optimization model incorporating effective dispatch of DGs, as developed in this study, offers a practical solution for leveraging DG resources in DNs to support optimal planning and development of EVCS infrastructure in practical applications.

5. CONCLUSION

With verify simulation results, it can be concluded that the proposed MGO is well suited for solving the optimal EVCS siting problem in DNs. All investigated cases demonstrate the superior performance and strong adaptability of MGO in searching for optimal solutions under both scenarios, namely without spatial constraints and with spatial installation constraints on EVCS deployment. The simulation outcomes obtained using MATLAB R2022a confirm the suitability of the proposed optimization model in achieving the objectives of minimizing power losses, maintaining bus voltage stability, and satisfying power balance constraints. Notably, the EVCS siting problem incorporating spatially differentiated capacity constraints exhibits greater flexibility in EVCS load allocation and enables more effective utilization of distributed generators within the DN. This approach contributes to improved operational stability and overall system efficiency. Therefore, the proposed model provides a practical and reliable solution for calculation, planning, and development of EVCS infrastructure in real world DNs.

ACKNOWLEDGMENT

The authors would like to sincerely acknowledge Can Tho University of Engineering and Technology and Ho Chi Minh City University of Technology, Vietnam National University Ho Chi Minh City, for their support of this research.

REFERENCES

[1] P. M. Forster *et al.*, “Indicators of Global Climate Change 2023: annual update of key indicators of the state of the climate system and human influence,” *Earth Syst. Sci. Data*, vol. 16, no. 6, pp. 2625–2658, Jun. 2024, doi: https://doi.org/10.5194/ESSD-16-2625-2024.

[2] F. Xolmurotov *et al.*, “the Impact of Renewable Energy Consumption on Unemployment Rates in Uzbekistan: an Ardl Approach,” *Environ. Econ.*, vol. 16, no. 1, pp. 78–88, 2025, doi: https://doi.org/10.21511/ee.16(1).2025.06.

[3] M. T. Hossain, S. I. Khan, and Z. Al Dodaev, “A Comprehensive Study of Effects of Renewable Energy Based Electric Vehicles on Environment,” *Control Syst. Optim. Lett.*, vol. 2, no. 2, pp. 234–240, 2024, doi: https://doi.org/10.59247/csol.v2i2.100.

[4] P. Bhosale, A. Sujil, R. Kumar, and R. C. Bansal, “Electric Vehicle Charging Infrastructure, Standards, Types, and Its Impact on Grid: A Review,” *Electr. Power Components Syst.*, pp. 1–25, 2024, doi: https://doi.org/10.1080/15325008.2024.2315206.

[5] M. Katontoka, F. Orsi, M. Bakker, and B. Hocks, "International Journal of Sustainable Transportation Toward sustainable transportation: A systematic review of EV charging station locations" 2025, doi: https://doi.org/10.1080/15568318.2025.2528085.

[6] D. Batic, V. Stankovic, and L. Stankovic, "Geodemographic aware electric vehicle charging location planning for equitable placement using Graph Neural Networks: Case study of Scotland metropolitan areas," *Energy*, vol. 324, p. 135834, Jun. 2025, doi: https://doi.org/ 10.1016/J.ENERGY.2025.135834.

[7] W. Morocho-Chicaiza, A. Barragán-Escandón, E. Zalamea-León, D. Ochoa-Correa, J. Terrados-Cepeda, and X. Serrano-Guerrero, "Identifying locations for electric vehicle charging stations in urban areas through the application of multicriteria techniques," *Energy Reports*, vol. 12, pp. 1794–1809, Dec. 2024, doi: https://doi.org/10.1016/J.EGYR.2024.07.057.

[8] J. Zhang, W. Jing, Z. Lu, H. Wu, and X. Wen, "Collaborative strategy for electric vehicle charging scheduling and route planning," *IET Smart Grid*, vol. 7, no. 5, pp. 628–642, Oct. 2024, doi: https://doi.org/10.1049/STG2.12170.

[9] C. Y. Hsu *et al.*, "Multi-Objective Particle Swarm Optimization Algorithm for Optimal Placement of Electric Vehicle Charging Stations in Distribution System," *Energy Sci. Eng.*, 2025, doi: https://doi.org/10.1002/ESE3.70223.

[10] G. Fotis, "An improved arithmetic method for determining the optimum placement and size of EV charging stations," *Comput. Electr. Eng.*, vol. 120, p. 109840, Dec. 2024, doi: https://doi.org/10.1016/J.COMPELECENG.2024.109840.

[11] F. Rahmat Astianta Bukit, H. Zulkarnain, and C. Purnama Kusuma, "Optimizing electric vehicle charging station placement integrates distributed generations and network reconfiguration," *Int. J. Electr. Comput. Eng.*, vol. 14, no. 5, pp. 4929–4939, 2024, doi: https://doi.org/10.11591/ijece.v14i5.pp4929-4939.

[12] T. Yuvaraj, K. R. Devabalaji, S. B. Thanikanti, V. B. Pamshetti, and N. I. Nwulu, "Integration of Electric Vehicle Charging Stations and DSTATCOM in Practical Indian Distribution Systems Using Bald Eagle Search Algorithm," *IEEE Access*, vol. 11, pp. 55149–55168, 2023, doi: https://doi.org/10.1109/ACCESS.2023.3280607.

[13] M. Bilal and M. Rizwan, "Integration of electric vehicle charging stations and capacitors in distribution systems with vehicle-to-grid facility," *Energy Sources, Part A Recover. Util. Environ. Eff.*, vol. 47, no. 1, pp. 7700–7729, 2025, doi: https://doi.org/10.1080/15567036.2021.1923870.

[14] N. Dharavat, S. K. Sudabattula, and V. Suresh, "Optimal Integration of Distributed Generators (DGs) Shunt Capacitors (SCs) and Electric Vehicles (EVs) in a Distribution System (DS) using Marine Predator Algorithm," *Int. J. Renew. Energy Res.*, vol. 12, no. 3, pp. 1637–1650, 2022, doi: https://doi.org/10.20508/ijrer.v12i3.13230.g8550.

[15] P. Mallikarjun, S. R. G. Thulasiraman, P. K. Balachandran, and M. A. A. M. Zainuri, "Economic energy optimization in microgrid with PV/wind/battery integrated wireless electric vehicle battery charging system using improved Harris Hawk Optimization," *Sci. Rep.*, vol. 15, no. 1, pp. 1–30, 2025, doi: https://doi.org/10.1038/s41598-025-94285-7.

[16] D. N. Araujo *et al.*, "Optimum design of on-grid PV-BESS for fast electric vehicle charging station in Brazil," *2021 IEEE PES Innov. Smart Grid Technol. Conf. - Lat. Am. ISGT Lat. Am. 2021*, Sep. 2021, doi: https://doi.org/10.1109/ISGTLATINAMERICA52371.2021.9543071.

[17] M. H. Alsharif, F. Alsaif, M. K. Singla, S. Manna, and M. K. Kim, "Techno-economic optimization and environmental analysis of a solar-powered Electric Vehicles (EVs)

charger system for a greener transportation ecosystem," *Energy Reports*, vol. 13, pp. 5803–5814, Jun. 2025, doi: https://doi.org/10.1016/J.EGYR.2025.05.040.

[18] M. A. Al-Betar, Z. A. A. Alyasseri, M. A. Awadallah, and I. Abu Doush, *Coronavirus herd immunity optimizer (CHIO)*, vol. 33, no. 10. Springer London, 2021. doi: https://doi.org/10.1007/s00521-020-05296-6.

[19] S. Sharma, "ICSCCC 2021 - International Conference on Secure Cyber Computing and Communications," *ICSCCC 2021 - Int. Conf. Secur. Cyber Comput. Commun.*, 2021.

[20] B. Abdollahzadeh, F. S. Gharehchopogh, N. Khodadadi, and S. Mirjalili, "Mountain Gazelle Optimizer: A new Nature-inspired Metaheuristic Algorithm for Global Optimization Problems," *Adv. Eng. Softw.*, vol. 174, no. August, p. 103282, 2022, doi: https://doi.org/10.1016/j.advengsoft.2022.103282.

[21] S. Saremi, S. Mirjalili, and A. Lewis, "Grasshopper Optimisation Algorithm: Theory and application," *Adv. Eng. Softw.*, vol. 105, pp. 30–47, 2017, doi: https://doi.org/10.1016/j.advengsoft.2017.01.004.

[22] I. Ahmadianfar, O. Bozorg-Haddad, and X. Chu, "Gradient-based optimizer: A new metaheuristic optimization algorithm," *Inf. Sci. (Ny).*, vol. 540, pp. 131–159, 2020, doi: https://doi.org/10.1016/j.ins.2020.06.037.

[23] S. Mirjalili, S. M. Mirjalili, and A. Lewis, "Grey Wolf Optimizer," *Adv. Eng. Softw.*, vol. 69, pp. 46–61, 2014, doi: https://doi.org/10.1016/j.advengsoft.2013.12.007.

[24] A. A. A. Mohamed, Y. S. Mohamed, A. A. M. El-Gaafary, and A. M. Hemeida, "Optimal power flow using moth swarm algorithm," *Electr. Power Syst. Res.*, vol. 142, pp. 190–206, 2017, doi: https://doi.org/10.1016/j.epsr.2016.09.025.